International Journal of Physics and Applications

E-ISSN: 2664-7583
P-ISSN: 2664-7575
Impact Factor (RJIF): 8.12
IJOS 2025; 7(2): 100-107

www.physicsjournal.in
Received: 06-05-2025
Accepted: 09-06-2025

Arkan G Salman
Laboratory of Nanomaterials and Plasma, College of Science, University of Thi-Qar, Thi Qar, Iraq

Majid R Al-bahrani
Laboratory of Nanomaterials and Plasma, College of Science, University of Thi-Qar, Thi Qar, Iraq

Corresponding Author:
Arkan G Salman
Laboratory of Nanomaterials and Plasma, College of Science, University of Thi-Qar, Thi Qar, Iraq

The optoelectronic properties of lead-free Cs_2NaBiI_6 double perovskites via Mg^{2+} doping

Arkan G Salman and Majid R Al-bahrani

DOI: https://doi.org/10.33545/26647575.2025.v7.i2b.174

Abstract
This study analyzes the structural and optical properties of Mg^{2+}-doped Cs_2NaBiI_6, synthesized through hydrothermal methods, paying special attention to magnesium additions. The nominal magnesium doping levels of 1%, 3%, and 5% were used. These were characterized using X-ray diffraction (XRD), Field Emission Scanning Electron Microscopy (FESEM), Transmission Electron Microscopy (TEM), and UV-Vis absorption spectroscopy. The results showed that the incorporation of Mg^{2+} ions improved crystallization processes by decreasing the energy band gap and increasing light absorption, especially at the 3% and 5% ratios, which also had a more dense and uniform structure. Furthermore, XRD analyses confirmed that the main crystalline phase was unchanged with only some evidence of secondary phase formation at the highest percent of blur. The findings indicate that the post incorporation of magnesium ion on Cs_2NaBiI_6 may enhance its efficiency as a potential photovoltaic sorbent, especially for solar cells due to its low environmental impact.

Keywords: Double perovskite, Cs_2NaBiI_6, XRD, FSEM, TEM, UV-Vis spectroscopy, band gap, photovoltaic material

1. Introduction
General-formula halide perovskites (ABX_3) represent one of the most promising materials in solar cells and semiconductors, with lead-based perovskites showing exceptional photovoltaic efficiency [1, 2, 3, 4]. From this standpoint, interest has emerged in the search for non-toxic alternatives that preserve perovskites in its distinctive properties. Bismuth is one of the most prominent alternatives proposed due to its low toxicity and affinity of its electronic properties to lead [5, 6, 7, 8, 9]. However, the difference in equivalence between bismuth (+3) and lead (+2) prevents bismuth from directly replacing lead in single-site perovskite (ABX_3) [10]. To overcome this dilemma, a strategy was adopted to build a double (double-site) perovskite, which combines bismuth (3^+) and one of the monovalent metals in a ratio of 1:1 at site B, to form $A_2B'B''X_6$ compounds, where B = Bi or Sb [11]. Within this framework, unleaded perovskites of the Cs_2NaBX_6 type (e.g. Cs_2NaBiX_6) were polarized. Great attention, as it meets the stability standards and optical properties required for photovoltaic and
The Cs_2NaBiI_6 compound is a prime example of lead-free double perovskite, which has received recent and intensive study. Research has shown that this compound has a relatively small optical energy gap (~1.66 electron volts), with high stability to moisture and oxygen in ambient conditions, making it a promising candidate as an absorbent layer in solar cells and optical sensors [12]. The crystal structure of Cs_2NaBiI_6 has been verified and classified into a double cubic structure similar to elpasolite [13], where Bi^{3+} and Na^+ ions alternately occupy the positions of the B lattice within the crystal structure represented by the general formula Cs_2NaBiI_6 [14]. This design compensates for Bi^{3+}'s high charge through a single-charge partner (Na^+), maintaining the balance of charges in the crystal lattice without the presence of toxic lead. The reconciliation of the appropriate energy gap with the chemical stability of this compound attracts the interest of researchers for its development and use in green optoelectronic applications [15] Figure 1.

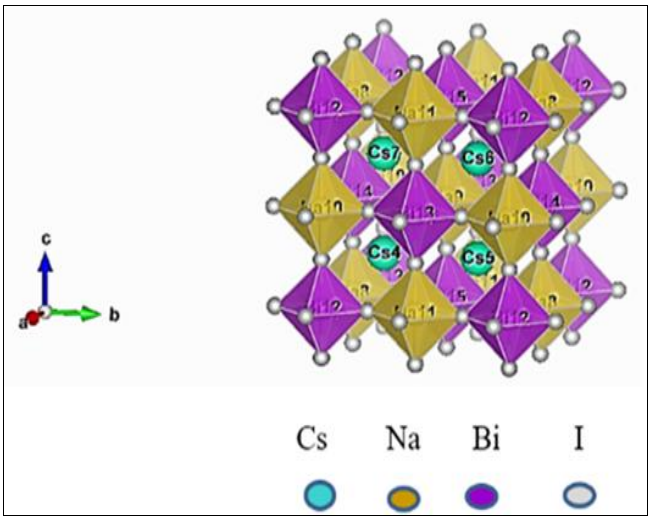

Fig 1: Proposed cubic structure of Cs2NaBiI6.Images are produced by VESTA software [16]

In addition to efforts to design lead-free perovskite materials, doping metals has emerged as an effective strategy to adjust and improve the electronic and optical properties of these materials. Experimental and theoretical studies have shown that the introduction of trace amounts of metal ions into the crystal lattice of perovskite compounds can cause substantial modifications in the structure, optical spectrum, and electrical properties of the material. For example, the study of Christians showed that modification of surface facades can enhance operational stability in uncoated solar cells, while the Grätzel study [17] discussed the effect of material installation on photovoltaic performance. Jeon *et al.* [18] have shown through direct experience that optimizing preparation conditions affects the absorption properties and charge transfer in thin films. For example, a study showed that perovskite grafted methylammonium lead iodide ($MAPbI_3$) with 1% magnesium (Mg^{2+}). This led to enhanced crystalline growth in the prepared film increasing the surface structure homogeneity by the reduction of fine imperfections and holes. [19, 16]. An electronic structure change of the material was also noted due to the decrease in valence band position which improved the performance and stability of the solar cell under high humidity conditions. This aligns with Fakhruddin and coworkers in his research on magnesium $MAPbI_3$ grafting where their findings indicated these structural alterations increased cell efficiency and stable performance under high humidity conditions [20].

This work is centered on the assumption that attaching selectively chosen metal ions can increase absorption within the visible spectrum and lower the energy gap of lead-free double perovskite's optical properties. One of the recent works demonstrated that substituting bismuth ions (Bi^{3+}) with iron ions (Fe^{3+}) in $Cs_2NaBiCl_6$ showed a notable increase of the electron density neighboring the Valence Band Maximum (VBM) which positively impacted the material's photoelectric properties. UV-Vis and XRD measurements, DFT calculations showed the changes due to grafting with considerable amount of striking alterations in the electronic structure were found to have grafted in photoabsorption and yield inside the electronic construction of the compound [21]. Focusing on this idea, this experimental study are intended to evaluate the impact of Mg ions with molar fractions - 1%, 3%, and 5% - on Cs_2NaBiI_6. Magnesium was selected due to its established ability in previous works to enhance optical and crystalline properties in similar systems and owing to the ionic radius of magnesium. The introduction of Mg^{2+} into the crystal lattice of Cs_2NaBiI_6 is expected to lead to changes in cell dimensions, rearrangement in ion sites, possible secondary phases, and potential effects on optical transition and energy gap.

The present study will be considered to clarify the role of Mg^{2+} composite on Cs_2NaBiI_6, based on the multipurpose of the data as well as the consistent and comprehensive data treatment. The analyses of X-Ray Diffraction (XRD) patterns will be conducted primarily to check the successful introduction of Mg^{2+} ions into the crystal lattice and to determine whether the original crystal phase still remained or whether changes occurred so that other crystal phases were formed with the increasing of the grafting rates involved [22]. The results of the microscope will also contribute. Field-Emission Scanning Electron (FESEM) and Transmission Electron Microscopy (TEM) show how magnesium affects particle size, crystal regularity, and degree of crystallization, enabling the link between microstructure and changes in optical properties [23]. UV-Vis spectroscopy data will be used to monitor changes in the absorption spectrum and determine whether magnesium inlay makes adjustments in the optical energy gap, either through displacements at the absorption edge or by introducing sub-energy levels within the electronic structure [24]. Taken together, these results will demonstrate the extent to which Mg^{2+} can improve the material's response to visible light or extend its spectrum absorption, which are critical factors for enhancing absorption efficiency in photovoltaic applications. Based on the above, this study is expected to contribute to providing an accurate scientific analysis of the effect of Cs_2NaBiI_6 grafting with magnesium and to determine the structural and visual effects of this modification. The results will also provide a model that can be rolled out to other perovskite systems, enhancing the potential for developing lead-free materials with high stability and improved efficiency, and compliant with sustainability and environmental standards in the field of optoelectronics and advanced solar energy [25].

Experimental section

Material and synthesis of Cs_2NaBiI_6

The target material was synthesized through a simple one-step hydrothermal process. The following materials were used: Cesium iodide (CsI, 99.99%) M.W=259.81 g/mol, CAS Number [7789-17-5], Sodium iodide (NaI, 99.99%) M.W=149.89 g/mol, CAS Number [7681-82-5], Bismuth iodide (BiI_3, 99.99%) M.W=589.69 g/mol, CAS Number [7787-64-6] Dimethyl sulfoxide (DMSO, 99.9%Sigma-Aldrich). To prepare Cs_2NaBiI_6 crystals by the hydrothermal method, the feedstock is first dissolved in the following molar ratios: two moles of cesium iodide (CsI), one mole of sodium iodide (NaI), and one mole of bismuth iodide (BiI_3), using a high-purity dimethyl sulfoxide solvent (DMSO). The dissolving process is carried out in a homogeneous medium with constant stirring and slight heating to a temperature of approximately 60 °C [26]. After the dissolution process is complete and a homogeneous and clear solution is obtained, the solution is carefully transferred to an autoclave with an inner layer of Teflon, and sealed well to ensure that the pressure produced during the reaction is withered. Next, place the reaction vessel in a preset oven at 120°C and leave for two full hours to complete the reaction. At the end of the reaction period, the heat is gradually reduced naturally and slowly until the vessel reaches laboratory temperature (approximately within 12 hours), in order to ensure good and uniform

crystallization. [27]. When cooling is complete, the vessel is opened, and the resulting crystals, which have a distinctive dark red color, are extracted. These crystals are then thoroughly washed using distilled water several times in order to get rid of any impurities or residues that may be on their surface. The crystals are then thoroughly dried in a vacuum oven at a moderate temperature of 40 to 60 °C. The resulting crystals are enhanced by recrystallization in a suitable solvent such as DMSO, with the aim of separating and removing secondary stages that may be bound to the compound [21].

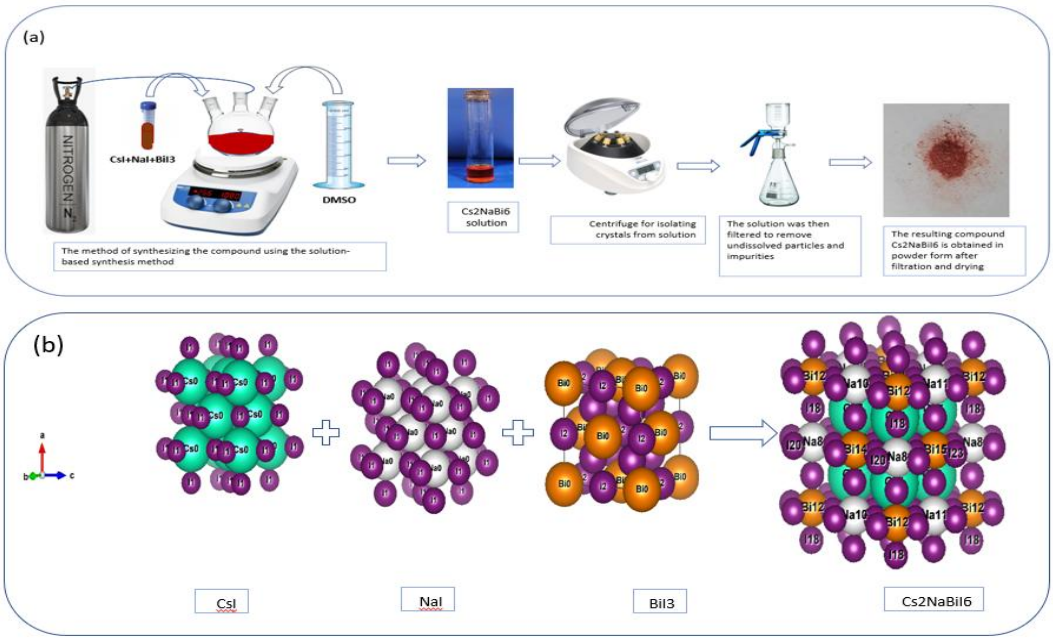

Fig 2: (a) Synthesis of the compound Cs_2NaBiI_6. (b) Each molecular structure is shown in a space-filling model, where: Cs atoms are cyan, Na atoms are white, Bi atoms are orange,I atoms are purple. The diagram shows these precursors combining to form the complex double perovskite structure of Cs_2NaBiI_6. Images are produced by VESTA software [16]

Results and Discussion

This research focused on the surface and morphological features of Cs_2NaBiI_6 composite membrane and its constituent materials, NaI, CsI, and BiI_3, employing Field Emission Scanning Electron Microscopy (FESEM) technology. It was found that Cs_2NaBiI_6 membrane has aspherical grains of small size that build up an almost smooth surface and that these grains are of a relatively uniform size and controlled spatial distribution phenomena of several nanometers which is indicative of favorable crystallization process control. Some small pores still need to be improved in sedimentation and annealing steps.

In comparison, NaI has a striking irregularity in both agglomerate size and grain size which may obstruct cargo transport. The surface structure of the polycrystalline CsI is smoother than that of granules, containing larger gaps or voids that may give rise to electronic malfunctions. BiI_3 membrane is characterized by its porous structure composed of fragmentation, which depicts the rate of crystallization and determines the order of the membrane towards charge reclamation. Therefore, among the investigated materials, Cs_2NaBiI_6 demonstrated the most favorable structural and morphological features, which increases the applicability of the material in stable, lead-free photovoltaic systems.

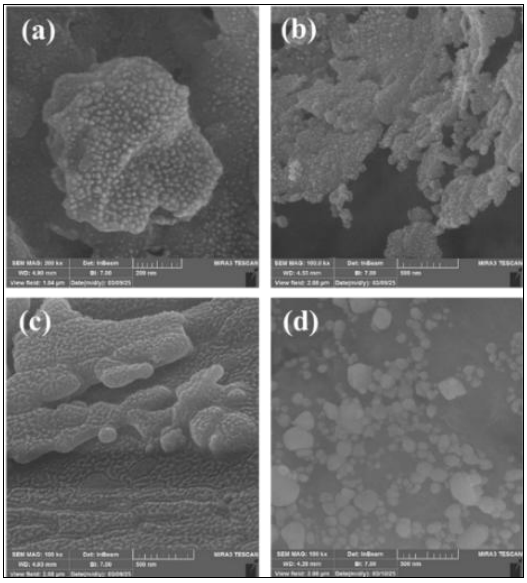

Fig 3: FESEM Images of, (a) Cs_2NaBiI_6, (b) NaI, (c) CsI and (d) BiI_3

A Transmission Electron Microscopy (TEM) study was conducted on Cs_2NaBiI_6, NaI, CsI, and BiI_3 nanoparticles to assess their morphological attributes and evaluate their potential roles within Perovskite Solar Cell (PSC) architectures. These nanomaterials demonstrated diverse shapes, size distributions, and aggregation behaviors. Cs_2NaBiI_6 nanoparticles exhibited dense secondary agglomerates, composed of well-defined spherical primary particles ranging from 20-50 nm. While aggregation may pose challenges for uniform film deposition, the consistent nanocrystalline morphology and high atomic number make Cs_2NaBiI_6 a promising candidate for lead-free PSC absorbers with potential radiation stability and enhanced photon absorption.

NaI nanoparticles revealed uniform, monodisperse spherical morphology with diameters between 10 and 30 nm and showed excellent colloidal stability with no significant agglomeration. Such layers are known to reduce defect states and improve power conversion efficiency. CsI nanoparticles displayed elongated, rod-like structures with lengths between 40 and 120~nm and widths of 20-50 nm. BiI_3 nanoparticles demonstrated heterogeneous morphologies, including plate-like and rod-shaped structures, with widths ranging from 30 to 100 nm and lengths extending up to 200~nm. These morphological traits make BiI_3 a suitable candidate for planar or layered PSC configurations, where directional charge transport and anisotropic electronic properties are beneficial Figure 4.

Analysis using X-Ray diffraction (XRD) of Cs_2NaBiI_6 showed clear and prominent reflections at angle values (2θ) of approximately 14.5°, 20.7°, 28.5°, 33.1°, 41.2° and 50.3°, and these reflections are characterized by narrow and sharp peaks indicating a high-quality crystal structure and double cube symmetry, which confirms the successful formation of the target perovskite phase. The absence of any secondary reflections or impurities highlights the purity of the phase and indicates excellent crystal uniformity, which reflects positively on the properties of the material related to electronic transmission and photoelectric efficiency. In contrast, the NaI composite in XRD has shown reflections of large amplitude and low intensity, especially near the 27° angle, which is usually attributed to the crystal plane (200) of the cubic structure centered on faces (FCC). This amplitude indicates a low degree of crystallization, possibly the presence of amorphous or turbulent regions within the crystal lattice.

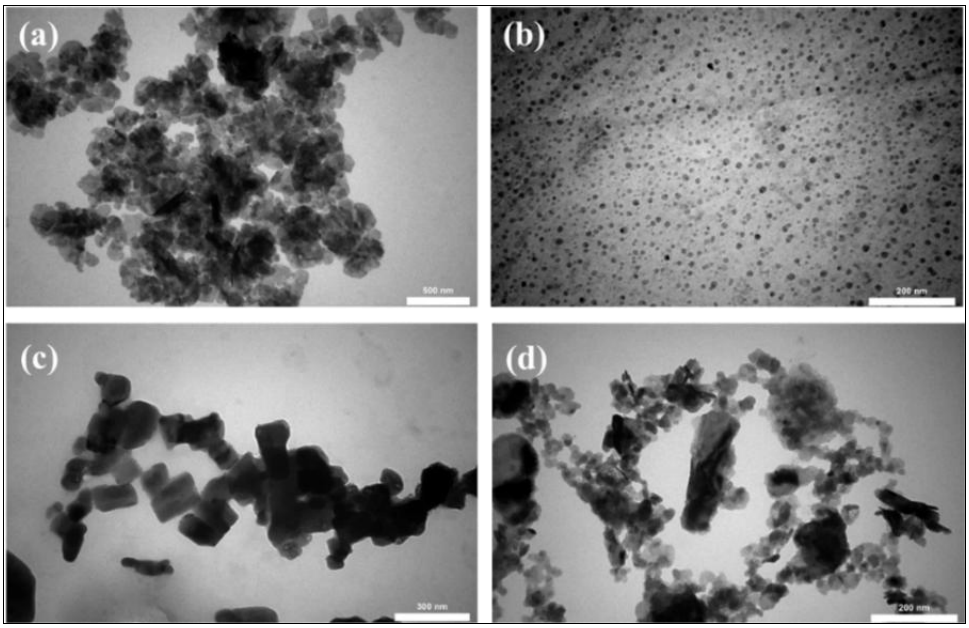

Fig 4: TEM Images of, (a) Cs_2NaBiI,(b) NaI, (c) CsI and (d) BiI_3

CsI analysis showed sharp and clear peaks, particularly at angle 2θ ≈ 30°, confirming the cubic structure of the halide, which has a good degree of crystallization and stability, making it suitable for use in radiation detection applications.

BiI_3 exhibited a characteristic pattern of intense reflections at the angle 2θ ≈ 28°, which corresponds to the crystal plane (003) of its rhombic system structure, confirming its high crystallization and making it of great importance in optoelectronic applications and optical detectors. Based on these results, it is clear that Cs_2NaBiI_6 has a remarkable superiority in terms of crystallization quality and phase purity compared to its primary components (CsI, NaI, BiI_3), making it a promising material for use as a stable and lead-free alternative in future solar cell technologies and photovoltaic applications in general Figure 5.

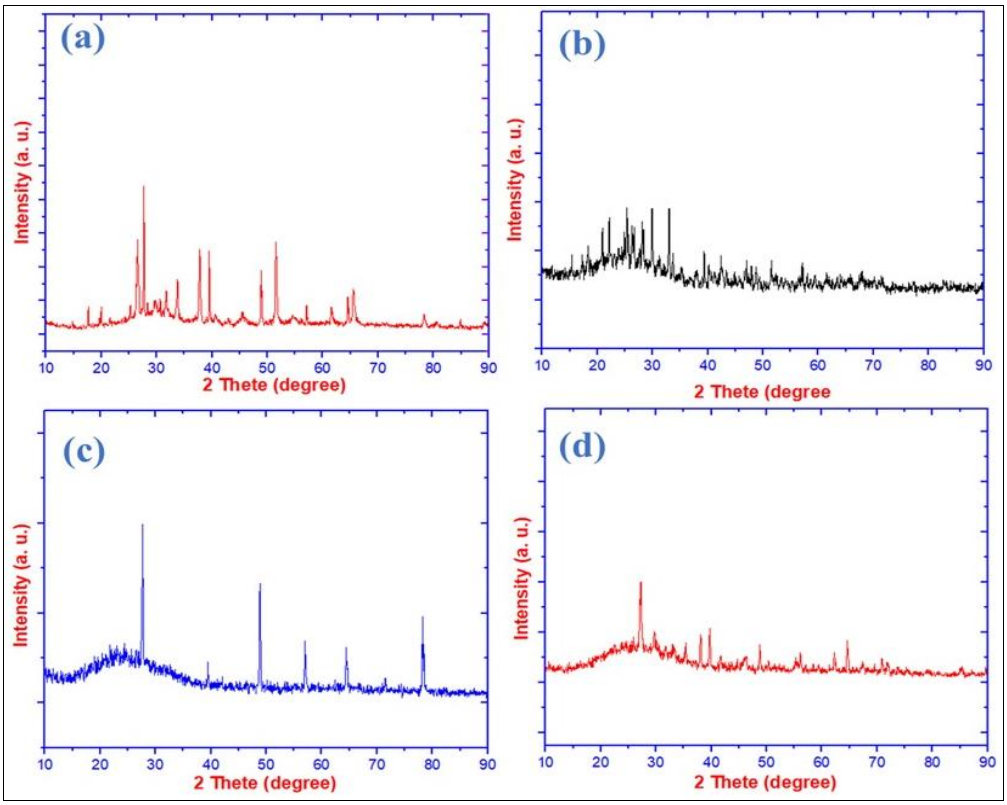

Fig 5: (XRD) patterns of, (a) Cs_2NaBiI_3, (b) NaI, (c) CsI and (d) BiI_3

Cs_2NaBiI_6 (CNBI): Broad absorbance in the UV-visible region (200-600 nm), indicating a significant band edge and possibly a smaller optical band gap suitable for visible-light absorption. The curve suggests semiconducting behavior, relevant for optoelectronic or photovoltaic applications. NaI: Sharp absorption below 250 nm with negligible absorbance in the visible range, indicating a wide band gap and insulating behavior. CsI: Similar to NaI, showing strong absorbance below 250 nm, confirming its wide band gap and poor visible light absorption. BiI_3: Displays multiple absorption features in the UV region (200-400 nm), indicating some light absorption in the near-UV to UV-A range, consistent with a medium band gap (1.5-2 eV). CNBI shows enhanced visible light absorption compared to its precursors, suggesting successful formation of a new phase with improved optoelectronic properties. The precursor salts (NaI and CsI) mainly absorb in the deep UV, while BiI_3 contributes more to UV-visible absorption due to its narrower band gap Figure 6.

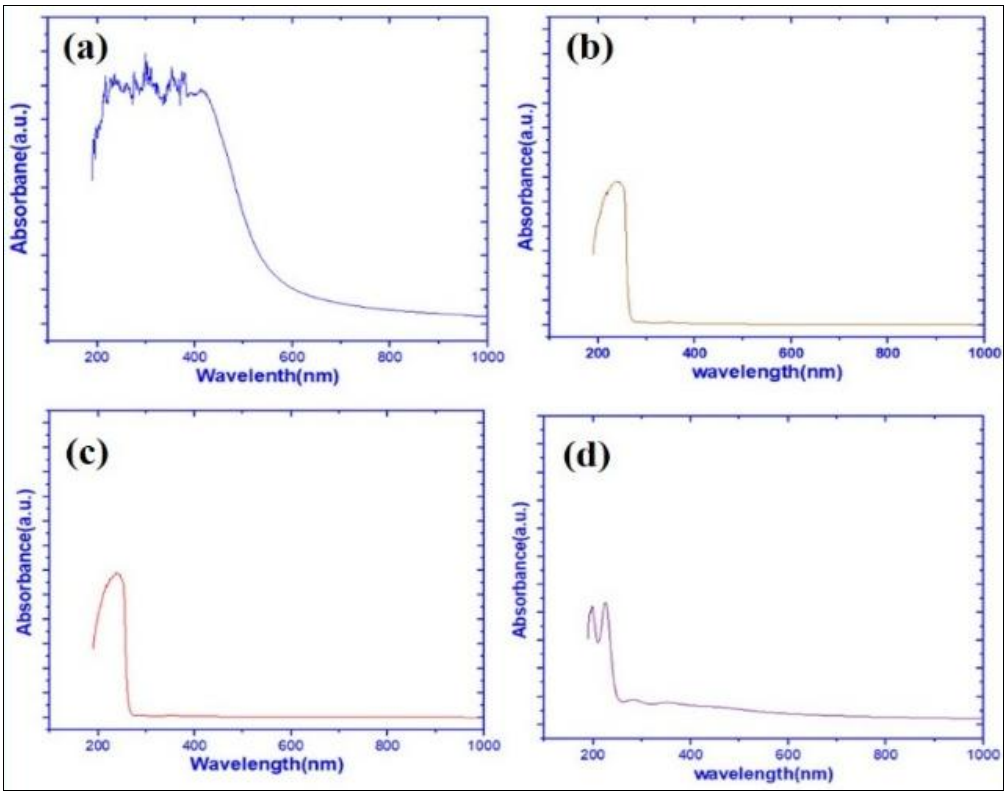

Fig 6: The UV-Vis spectrum showing absorbance curves for the four materials:(a) Cs_2NaBiI_6, (b) NaI, (c) CsI and (d) BiI_3

Field Emission Scanning Electron Microscopy (FE-SEM) images showed visible changes in the surface structure of Cs_2NaBiI_6 when smeared with different percentages of Mg. At 1% Mg, the structure appeared rough and irregular, indicating poor crystallization. By increasing the percentage to 3%, more uniform and homogeneous crystals emerged. At 5% Mg, a smooth and compact stratified structure was observed, reflecting a significant improvement in crystallization and structural stability. These results indicate that the coating of Cs_2NaBiI_6 with magnesium promotes crystal growth and improves morphological properties, which may reflect positively on the optical and photoelectric performance of the material Figure 7.

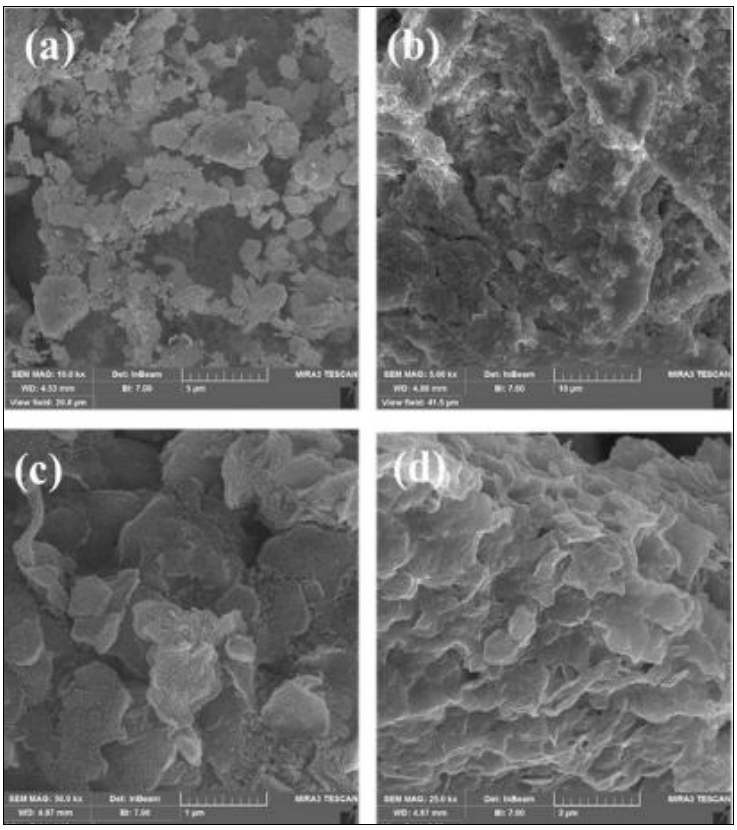

Fig 7: (FE-SEM): (a) Pure Mg (b) Daubing 1% Mg (c) Daubing 3% Mg (d) Daubing 5% Mg

TEM images showed that the impurity of the Cs_2NaBiI_6 compound with magnesium significantly affects the size, shape, and distribution of nanoparticles. As the concentration of mg increases, the nanostructure improves, and the degree of regularity and crystallization increases. This development in nanosynthesis may improve the optical and electronic properties of the composite, enhancing its efficiency in photovoltaic applications such as solar cells. Figure8.

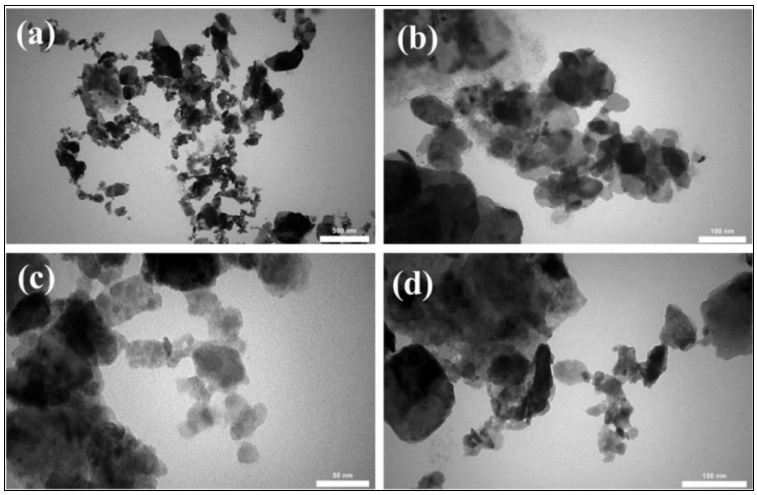

Fig 8: (TEM): (a) Pure Cs_2NaBiI_6 (b) Daubing 1% Mg (c) Daubing 3% Mg (d) Daubing 5% Mg

X-ray diffraction results showed that the magnesium Cs_2NaBiI_6 impurity affects the crystal structure. At 1% and 3% mg, doping contributed to improved crystallization and increased peak intensity, indicating an improvement in structure quality. At 5%, there were signs of secondary phase formation or deterioration in crystal regularity. These results indicate that the optimal percentage of Mg smearing is between 1% and 3% to obtain a stable and coherent crystal structure.

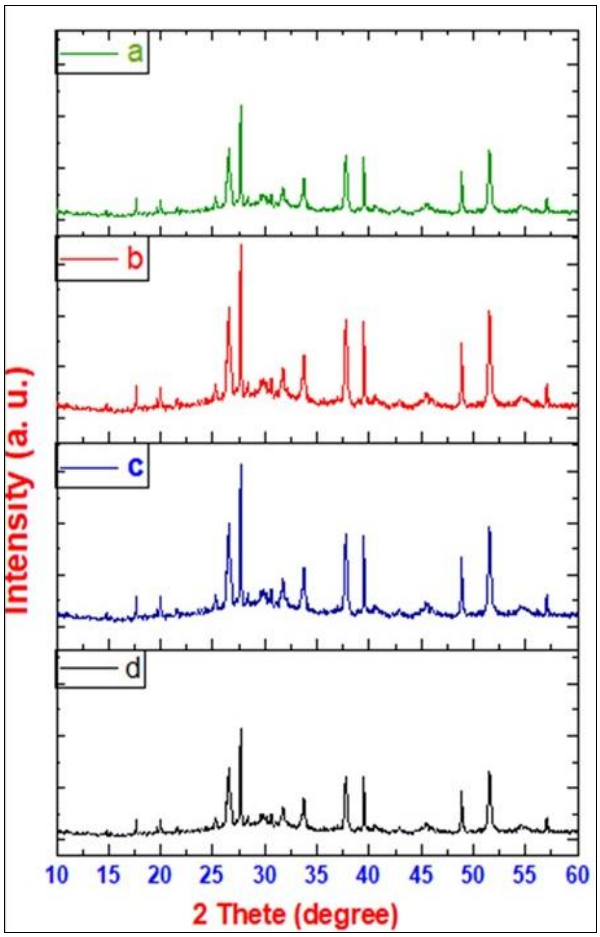

Fig 9: (XRD patterns): (a) Pure Cs_2NaBiI_6 (b) Daubing 1% Mg (c) Daubing 3% Mg (d) Daubing 5% Mg

UV-Vis spectra showed that the distortion of the Cs_2NaBiI_6 compound with magnesium leads to a gradual shift in the edge of the photo absorption towards longer wavelengths (Red Shift), reflecting a modification in the electronic structure and a gradual reduction in the optical energy gap. Improved absorption also indicates an increased effectiveness of the compound in capturing visible light. Figure 10.

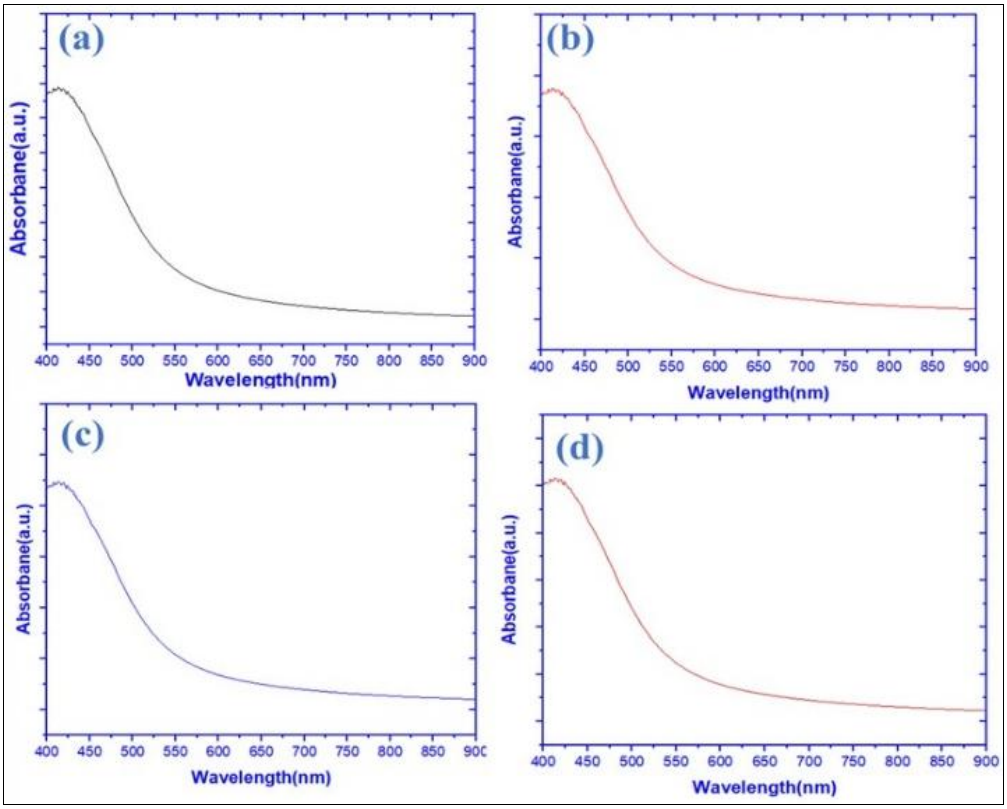

Fig 10: (UV-V): (a) Pure Cs_2NaBiI_6 (b) Daubing 1% Mg (c) Daubing 3% Mg (d) Daubing 5% Mg

Conclusions

The study of the effect of Cs_2NaBiI_6 champing with magnesium ions (Mg^{2+}) showed that the introduction of trace magnesium (up to 5%) leads to significant improvements in the structural and optical properties of the compound. FE-SEM and TEM images showed a clear improvement in the regularity and crystallization of the nanostructure with an increase in the Mg ratio, demonstrating stimulation of crystal growth and reduction of surface defects. XRD measurements showed that the best improvement in crystallization and crystal density was achieved at 3%, while 5% led to secondary phases that may affect structure uniformity. UV-Vis spectroscopy showed a gradual red shift at the absorption edge with an increase in magnesium, indicating a narrowing of the energy gap and enhancing the compound's ability to absorb visible light. The results prove that Cs_2NaBiI_6 doping with magnesium ions can be used as an effective mechanism for adjusting the electronic and optical structure, qualifying it to be a promising candidate for alternative, high-efficiency, and environmentally friendly photovoltaic applications. The study recommends further research on finer distortion ratios and examining the effect of other elements to improve the stability and performance of these materials in future photovoltaic devices.

References

1. Ali HH. Preparation and characterization of ZnO NWs/graphene nanocomposite as an effective photoanode electrode for improving the performance of the dye-sensitized solar cells. Univ Thi-Qar J Sci. 2023;10(1):11-15.
2. Abdulsada ZR, Kadhim SB, AbdulAlmohsin SM, Abdulaali HS. High efficiency (22.46) of solar cells based on perovskites. Univ Thi-Qar J Sci. 2023;10(2):187-191.
3. Noel NK, Abate A, Stranks SD, Parrott ES, Burlakov VM, Goriely A, *et al*. Interfacial charge-transfer doping of metal halide perovskites for high performance photovoltaics. Energy Environ Sci. 2019;12(10):3063-3073.
4. Eperon GE, Stranks SD, Menelaou C, Johnston MB, Herz LM, Snaith HJ. Formamidinium lead trihalide: a broadly tunable perovskite for efficient planar heterojunction solar cells. Energy Environ Sci. 2014;7(3):982-988.
5. Hao F, Stoumpos CC, Cao DH, Chang RPH, Kanatzidis MG. Lead-free solid-state organic-inorganic halide perovskite solar cells. Nat Photonics. 2014;8(6):489-494.
6. Ajeel HA, Al-Bahrani MR. Enhancement of electric efficiency and structural phase change of CsPbBr3 caused by Ni^{2+} doping. Iraqi J Appl Phys. 2024;20(4).
7. Tubena NL, Al-Bahrani MR. Enhancement of power conversion efficiency for perovskite solar cells using ZnO-G-Ge as electron transport layer. Iraqi J Appl Phys. 2024;20(4).
8. Hussian SK, Al-Bahrani MR. Influence of SiO_2 nanoparticles on the structural, morphology, and optical properties of CsPbBr3 quantum dots. J Polym Compos. 2023;11(2):62-69.
9. Abd Ali RA, Al-Bahrani MR, Waried HH. Design and fabrication of TiO2/G nanocomposite as electron transport layer for perovskite QD solar cells. J Nanostruct. 2024;14(3):953-962.
10. Zhang C, *et al*. Design of a novel and highly stable lead-free Cs_2NaBiI_6 double perovskite for photovoltaic application. Sustain Energy Fuels. 2018;2(11):2419-2428. DOI:10.1039/c8se00154e.
11. Volonakis G, *et al*. Lead-free halide double perovskites via heterovalent substitution of noble metals. J Phys Chem Lett. 2016;7(7):1254-1259.
12. Noel NK, *et al*. Lead-free organic-inorganic tin halide perovskites for photovoltaic applications. Energy Environ Sci. 2014;7(9):3061-3068.
13. Zhang C, *et al*. Design of a novel and highly stable lead-free Cs2NaBiI6 double perovskite for photovoltaic application. Sustain Energy Fuels. 2018;2(11):2419-2428. DOI:10.1039/c8se00154e.
14. Stoumpos CC, *et al*. Ruddlesden-Popper hybrid lead iodide perovskite 2D homologous semiconductors. Chem Mater. 2016;28(8):2852-2867.
15. Xiao Z, Meng W, Wang J, Yan Y. Thermodynamic stability and defect chemistry of bismuth-based lead-free double perovskites. ChemSusChem. 2016;9(18):2628-2633.
16. Momma K, Izumi F. VESTA 3 for three-dimensional visualization of crystal, volumetric and morphology data. J Appl Crystallogr. 2011;44(6):1272-1276.
17. Christians JA, *et al*. Tailored interfaces of unencapsulated perovskite solar cells for >1,000 hours operational stability. Nat Energy. 2018;3(1):68-74.
18. Grätzel M. The light and shade of perovskite solar cells. Nat Mater. 2014;13(9):838-842.
19. Jeon NJ, Noh JH, Kim YC, Yang WS, Ryu S, Seok SI. Solvent engineering for high-performance inorganic-organic hybrid perovskite solar cells. Nat Mater. 2014;13(9):897-903.
20. Yang F, *et al*. Magnesium-doped MAPbI3 perovskite layers for enhanced photovoltaic performance in humid air atmosphere. ACS Appl Mater Interfaces. 2018;10(29):24543-24548.
21. Udavant R, *et al*. Lead-free solid state mechanochemical synthesis of Cs2NaBi1-xFexCl6 double perovskite: reduces band gap and enhances optical properties. Inorg Chem. 2023;62(12):4861-4871.
22. Cullity BD, Stock SR. Elements of X-ray diffraction. 3rd ed. England: Pearson Education; 2001.
23. Peter YU, Cardona M. Fundamentals of semiconductors: physics and materials properties. Berlin: Springer; 2010.
24. Tauc J. Optical properties and electronic structure of amorphous Ge and Si. Mater Res Bull. 1968;3(1):37-46.
25. Hadi S, Al-Khursan AH. Developing the performance of double quantum dot solar cell structure. Univ Thi-Qar J Sci. 2021;8(1):148-154.
26. Liu F. Structural and optical properties of highly emitting lead-free double perovskites; 2022.
27. Liu Y, Wang W, Xiao F, Xiong L, Ming X. Stability and optoelectronic property of lead-free halide double perovskite Cs2B′BiI6 (B′ = Li, Na and K). Chin Phys B. 2021;30(10). DOI:10.1088/1674-1056/ac05a5.